A Wave-Based Model for Mutual Coupling and Truncation in Finite Tapered-Slot Phased Arrays

A.O. Boryssenko*, D.H. Schaubert
University of Massachusetts, Amherst, USA

C. Craeye
University Catholique de Louvain, Belgium

The tapered-slot (Vivaldi) endfire element is a promising candidate for broadband phased arrays. These arrays often are designed by using estimates from infinite arrays and ignoring edge effects arising from truncation of the infinite periodic array. However, the strong mutual coupling that contributes to wide bandwidth performance often leads to severe truncation effects within the finite Vivaldi array [1]. This study presents a time-domain approach to coupling and truncation phenomena with the help of (1) full-wave numerical simulation and (2) wave-based physical modeling. First, the full-wave solution provides the terminal currents for all elements in the finite array. Next, the coupling and truncation effects are modeled by waves propagating across the aperture. Time gating of the computed terminal currents enables decomposition of the wave events. The dispersion characteristics of the waves propagating across the aperture can be quantified and edge reflection coefficients can be estimated. This process provides physical insight to better understand the behavior of finite Vivaldi arrays.

Method of analysis

A time-domain integral equation (TDIE) solver [2] is applied to single-polarized dielectric-free Vivaldi arrays, Fig. 1. The element geometry, which is optimized for bandwidth and scanning in an infinite array, was simulated for several finite Vivaldi arrays by using TDIE and a frequency-domain technique with good agreement [3]. The TDIE code efficiently analyzes such finite arrays in active (Fig. 2a) and passive (Fig. 2b) modes. In the passive mode, the source is applied to a particular port while others are passively terminated. Short-circuit terminations are used here and the terminal current is computed for all other antenna ports. The terminal admittance matrix, which enables computation of passive and active input impedances (Fig. 2c), is calculated by repeating the computations with the generator applied to each of the array elements. Moreover, because the entire time histories of all terminal currents are available, wave phenomena can be effectively studied through the time gating technique.

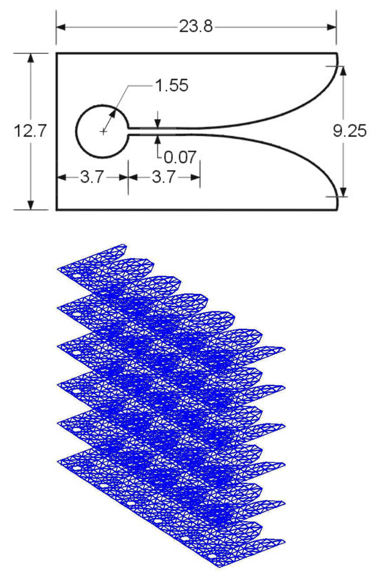

Fig. 1. Geometry of element and array. Array is comprised of elements on 12.7-cm square grid.

0-7803-7846-6/03/$17.00 ©2003 IEEE

Some numerical results

For demonstration of the proposed technique, 10x1 (E-plane) and 1x10 (H-plane) phased arrays are considered. Self-admittances and a few mutual admittances are plotted in Figs. 3 and 4. Based on the magnitude of the mutual admittances, the E-plane array has the stronger coupling because of direct electrical connection between the elements. The H-plane array coupling is weaker and, in fact, the self-admittance of the element (1,1) is similar to an isolated element of the same geometry.

A wave model is proposed to describe the coupling. When the end element (01-01) of the 10x1 or 1x10 array is excited by a gauss-derivative source, a wave propagates along the array and excites each element. Figs. 5a and 6a show the terminal currents. Under the assumption that only a single mode exists (probably valid except at higher frequencies of the operating band), the wave's complex propagation constant $\gamma = j\alpha + \beta$ is computed by using the Fourier transform applied to the portions of waveforms selected by the time gates shown in Figs. 5a and 6a. The width of the time window captures the essential wave characteristics and avoids reflection from the opposite edge of the array. To avoid strong influences from the generator, the propagation constant is computed by using only passive elements, e.g., elements 2, 3 and 4.

The propagation constants shown in Figs. 5b and 6b correspond propagation from elements 2 to 3 and 3 to 4. These two wave attenuation constants agree well above 0.4 GHz. The phase constants for the E-plane array differ somewhat below 0.6 GHz, but generally agree. The phase constant for the H-plane array is greater than free space (slow wave) up to the onset of grating lobes at 1.18 GHz.

Fig. 7 demonstrates use of the wave model and time gating to extract truncation effects in a finite array. Fig. 7a shows the passive input resistance and reactance of a central element computed by using the complete terminal current time history and a time-gated version that eliminates all edge reflections. Figs. 7b and 7c show the evolution of the finite-array input impedance through extension of the time gate to include the first-bounce and second-bounce reflections.

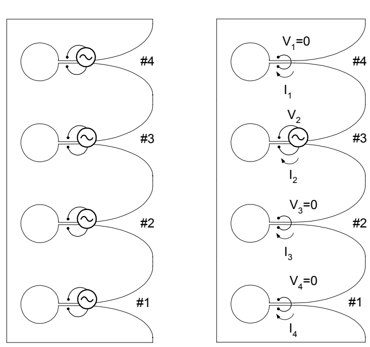

(a) (b)

Active Mode

$$Z^{active}_{inp\,\mathrm{i,j}} = Z_{i,j} + \sum_{\substack{m,n \\ i \neq m \\ \mathrm{j} \neq \mathrm{n}}} Z_{m,n} \cdot I_{m,n} / I_{i,j}$$

Passive Mode

$$Z^{passive}_{inp\,\mathrm{i,j}} = Y^{-1}_{\mathrm{i,j}} \qquad Y_{\mathrm{i,j}} = I_i / V_j$$

where

$$[Z] = [Y]^{-1}$$

(c)

Fig. 2. Vivaldi array in active (a) and passive (b) modes with related impedance expressions (c).

References

[1] H. Holter, and H. Steyskal, On the Size Requirement for Finite Phased-Array Model, *IEEE Transaction on Antennas and Propagation*, Vol. AP-50, No. 6, June 2002, pp. 836-840.

[2] A.O. Boryssenko, D.H. Schaubert, Time-Domain Integral-Equation-Based Solver for Transient and Broadband Problems in Electromagnetics, *The AMEREM 2002 Symposium*, Annapolis, MD, June 2-7, 2002, pp. 1-11.

[3] C. Craeye, A.O. Boryssenko, D.H. Schaubert, Analysis of Infinite and Finite Arrays of Tapered-Slot Antennas for SKA, *Proceedings of the 32nd European Microwave Week*, Milan, Italy, September 23 - 24, 2002, pp. 1003-1006.

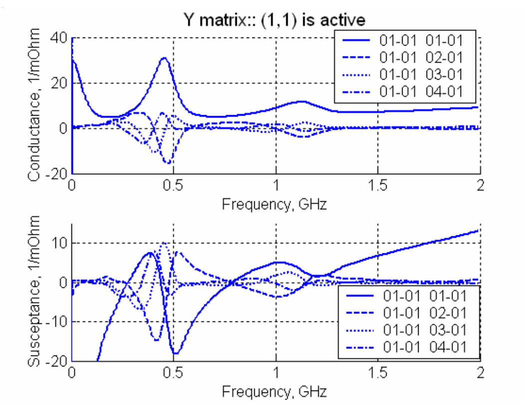

Fig. 3. 10x1 E-plane array admittances. Self-admittance of end element (01-01,01-01) and mutual admittance to neighboring elements 2, 3 and 4.

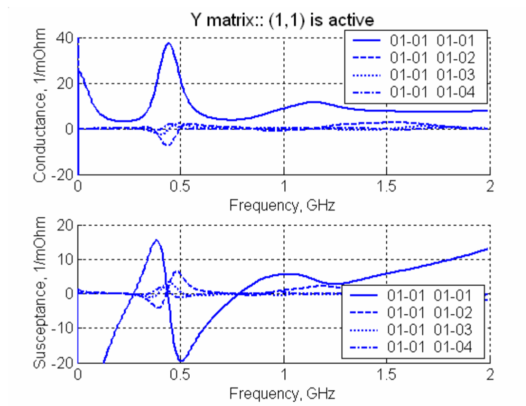

Fig. 4. 1x10 H-plane array admittances. Self-admittance of end element and mutual admittances to neighboring elements.

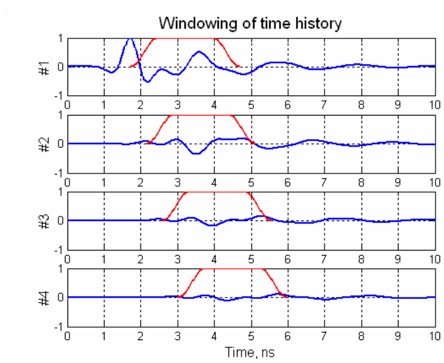

(a)

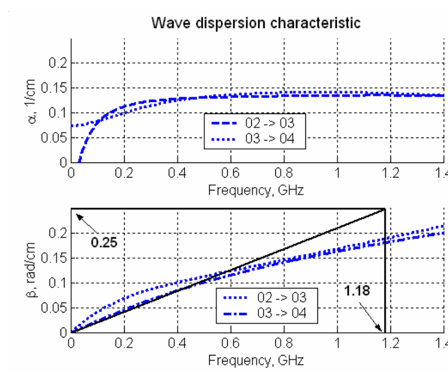

(b)

Fig. 5. 10x1 E-plane Vivaldi array with edge element driven by Gaussian-derivative pulse. (a) Terminal currents and time gates. (b) Propagation constant, assuming single mode.

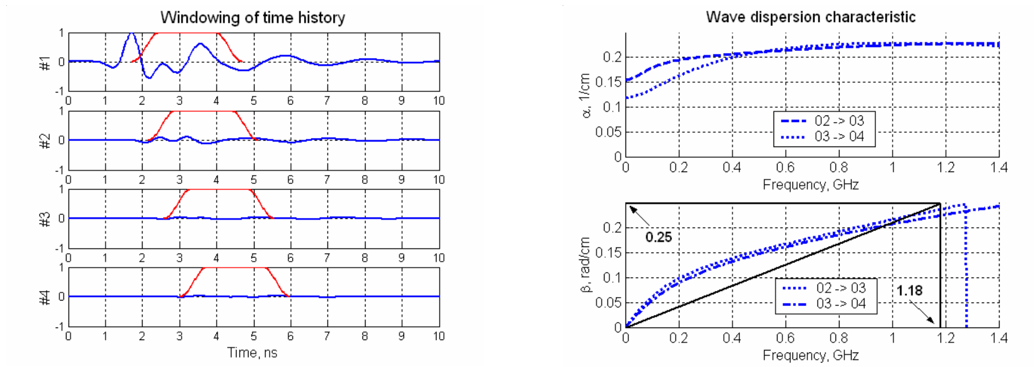

(a) (b)

Fig. 6. 1x10 H-plane Vivaldi array with edge element driven by Gaussian-derivative pulse. (a) Terminal currents and time gates. (b) Propagation constant, assuming single mode.

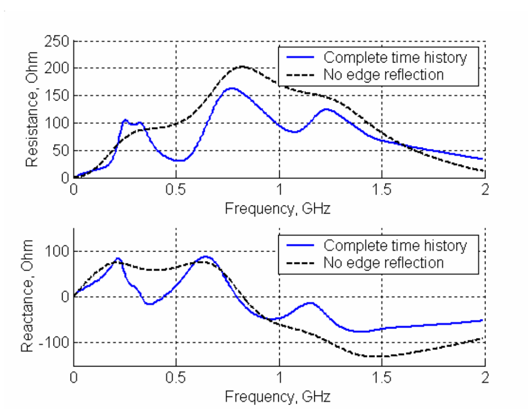

(a)

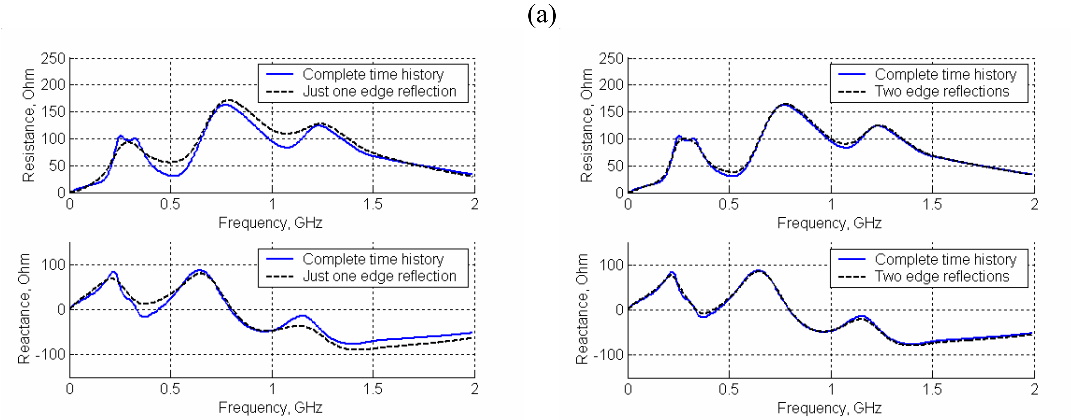

(b) (c)

Fig. 7. Passive input impedances for central element (05-01) in 10x1 E-plane Vivaldi array.